

EEG-based Emotion Style Transfer Network for Cross-dataset Emotion Recognition

Yijin Zhou¹, Fu Li¹, Yang Li^{*1}, Youshuo Ji¹, Lijian Zhang², Yuanfang Chen², Wenming Zheng³, Guangming Shi¹

¹Key Laboratory of Intelligent Perception and Image Understanding of Ministry of Education, the School of Artificial Intelligence, Xidian University, Xi'an, China.

²Beijing Institute of Mechanical Equipment, Beijing, China.

³Key Laboratory of Child Development and Learning Science (Ministry of Education), School of Biological Sciences and Medical Engineering, Southeast University, Nanjing, Jiangsu, China.

(*Corresponding author: Yang Li (E-mail: liy@xidian.edu.cn).)

Abstract

As the key to realizing aBCIs, EEG emotion recognition has been widely studied by many researchers. Previous methods have performed well for intra-subject EEG emotion recognition. However, the style mismatch between source domain (training data) and target domain (test data) EEG samples caused by huge inter-domain differences is still a critical problem for EEG emotion recognition. To solve the problem of cross-dataset EEG emotion recognition, in this paper, we propose an EEG-based Emotion Style Transfer Network (E²STN) to obtain EEG representations that contain the content information of source domain and the style information of target domain, which is called stylized emotional EEG representations. The representations are helpful for cross-dataset discriminative prediction. Concretely, E²STN consists of three modules, i.e., transfer module, transfer evaluation module, and discriminative prediction module. The transfer module encodes the domain-specific information of source and target domains and then re-constructs the source domain's emotional pattern and the target domain's statistical characteristics into the new stylized EEG representations. In this process, the transfer evaluation module is adopted to constrain the generated representations that can more precisely fuse two kinds of complementary information from source and target domains and avoid distorting. Finally, the generated stylized EEG representations are fed into the discriminative prediction module for final classification. Extensive experiments show that the E²STN can achieve the state-of-the-art performance on cross-dataset EEG emotion recognition tasks.

Introduction

As a new way of human-computer interaction in the 21st century, brain-computer interface (BCI) technology provides a new means of communication for us under the hot metaverse background (Guo and Gao 2022). Emotion plays a very significant role in human-computer interaction, which has led to the great attention of affective Brain-Computer Interfaces (aBCIs) in the interdisciplinary fields (Fiorini

et al. 2020; Katsigiannis and Ramzan 2018). Traditional aBCIs mainly rely on two mediums, behavioral signals and physiological signals, for emotion recognition (He et al. 2020). Compared with behavioral signals such as facial expressions, speech, and text, it is more reliable to distinguish the spontaneous emotion state through physiological signals such as electrocardiogram (ECG), electrooculogram (EOG), electromyogram (EMG), and electroencephalogram (EEG) (Zheng, Zhu, and Lu 2017; Song et al. 2021). Among them, EEG signals generated in the cerebral cortex are most associated with spontaneous emotional states (He et al. 2020; Shu and Wang 2017). With the development of wearable non-invasive EEG acquisition equipment in recent years, more and more researches have focused on the field of EEG-based emotion recognition.

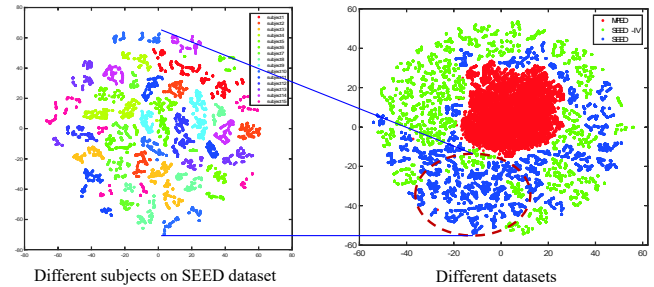


Figure 1: Distribution of EEG data in different subjects and datasets.

The previous EEG emotion recognition mainly focuses on intra-subject tasks (Xiao et al. 2022). For instance, Zheng et al. trained deep belief networks (DBNs) with differential entropy (DE) features of SEED dataset and achieved advanced results (Zheng and Lu 2015). Song et al. proposed the attention-long short-term memory (A-LSTM) to extract more discriminative features from multiple time-frequency domain features (Song et al. 2019). Peng et al. proposed a self-weighted semi-supervised classification (SWSC) model that utilizes a self-weighted variable to adaptively and quantitatively learn the importance of EEG features for cross-

session emotion pattern recognition (Peng et al. 2021). Zhong et al. proposed a regularized graph neural network (RGNN) that considers the biological topology among different brain regions to capture the local and global relationships between different EEG channels, which achieves advanced performance in cross-subject experiments on SEED and SEED-IV datasets (Zhong, Wang, and Miao 2020). Although various EEG emotion recognition methods have been proposed in the past several years, there are still some major issues that should be well investigated to further promote EEG emotion recognition. The first issue is the protocol for EEG emotion recognition. The existing protocols for EEG emotion recognition mostly are intra-subject and cross-subject EEG classification, in which the training and test EEG data come from the same experimental environment. How the performance varies between different experimental environments should be further studied, e.g., the cross-dataset EEG emotion recognition. To clearly and intuitively show the differences in the distribution of EEG data, we use the T-SNE technology to visualize the EEG data of different subjects in different datasets, as shown in Fig 1. Notably, there are significant differences in the distribution of EEG data among different subjects of the same dataset, and further, which are more prominent among diverse datasets.

The second issue is how to reduce the domain differences. Recently, several studies have attempted to address domain shifts in cross-subject EEG emotion recognition tasks. For example, BiDANN (Li et al. 2018) and TANN (Li et al. 2021) proposed by Li et al. have achieved advanced performance considering the distribution differences between training data and test data in the cross-subject EEG emotion recognition task. However, the inter-domain differences in cross-dataset EEG emotion recognition go well beyond that in the cross-subject EEG emotion recognition task, as shown in Fig. 1. Narrowing the differences between domains will further improve cross-dataset EEG emotion recognition and the generalization to new EEG emotional data. Therefore, overcoming the significant distribution divergence of EEG signals among different datasets is particularly challenging and promising for cross-dataset EEG emotion recognition.

To address the aforementioned issues, in this study, we propose an EEG-based Emotion Style Transfer Network (E^2STN) to obtain stylized emotional EEG representations containing emotion content of the source domain and statistical characteristics of the target domain, and meanwhile, make discriminative predictions for cross-dataset emotional EEG samples. E^2STN consists of three unique modules, namely the transfer module, the discriminative prediction module, and the transfer evaluation module. To realize the transfer of emotional EEG samples from the source domain to the target domain, we propose a transfer module to reorganize the emotional pattern information of the source domain and the statistical properties of the target domain into new stylized EEG representations. The first layer of the transfer module is two encoders corresponding to the source and target domains to extract their domain-specific information, namely the emotional content information of the source domain and the style statistics characteristics of the target domain. The decoder in the transfer module re-

combines emotional content and style characteristics to obtain stylized (transferred) emotional EEG representations. To make the stylized EEG representations contain more accurate emotional content information of the source domain and the statistical characteristic style of the target domain, we design a transfer evaluation module including content-aware loss, style-aware loss, and identity loss to constrain the process of transferring emotional EEG samples from the source domain to the target domain. The content-aware loss and style-aware loss in the transfer evaluation module ensure that the stylized representations can more precisely fuse two kinds of complementary information from source and target domains, respectively. A unique identity loss ensures that the transfer module is unbiased, i.e., the stylized representations remain unchanged when the source and target domains are the same samples. These losses are constructed from features extracted by the multi-layer convolution operations, which is inspired by (Gatys, Ecker, and Bethge 2016). The multi-layer convolutions explore the latent relationship between critical frequency bands and extract spatio-temporal information from the stylized representations, respectively. Finally, to extract deep features from both original (source domain) and stylized (transferred) EEG samples for discriminative predictions, we propose a discriminative prediction module that includes a dynamic graph convolutional network and two fully connected (FC) layers. The dynamic graph convolution network extracts spatial features from two types of samples, which are further fed into FC layers to generate discriminative class labels. A cross-entropy loss with the above transfer evaluation losses jointly optimizes the entire model to realize cross-dataset EEG emotion recognition from a global perspective.

Main contributions of this paper are summarized as three-fold:

- To our best knowledge, we propose an EEG-based Emotion Style Transfer Network (E^2STN) for the first time to obtain stylized emotional EEG representations for cross-dataset EEG emotion recognition. The model reorganizes the emotional content information of the source domain and the statistical characteristic style of the target domain into new stylized EEG representations, thereby further performing discriminative prediction of cross-dataset emotional EEG samples.
- The proposed E^2STN is implemented under the joint optimization of the cross-entropy loss and transfer evaluation losses. The transfer evaluation losses constrain the stylized EEG representations that can more precisely fuse two kinds of complementary information from source and target domains and avoid distorting, and meanwhile, the cross-entropy loss guides the discriminative prediction for cross-dataset EEG emotion recognition.
- Extensive experiments show that the proposed E^2STN can achieve the state-of-the-art performance on cross-dataset EEG emotion recognition tasks.

The rest of this paper is organized as follows. Section II summarizes a brief overview of related studies on EEG emotion recognition. Section III specifies the proposed E^2STN model in detail. Section IV discusses the results of the extensive experiments conducted. Finally, this paper is concluded

in Section V.

Related Work

Deep Learning in EEG Emotion Recognition

With the rapid development of deep learning, numerous studies have attempted to solve EEG emotion recognition using deep learning methods. For instance, Song et al. proposed a dynamical graph convolutional neural network (DGCNN) to recognize emotional EEG signals, which can dynamically learn the information transfer relationship between the nodes in a graph and achieve good results on SEED and DREAMER datasets (Song et al. 2020b). Considering the abundant spatial information in EEG signals, Song et al. proposed to convert multi-channel EEG signals into images for EEG emotion recognition, which converts the question of EEG-based emotion recognition into image recognition. To this end, they proposed a novel EEG-to-image method and a novel graph-embedded convolutional neural network (GECNN) method. Extensive experiments on four datasets have proved the effectiveness of GECNN (Song et al. 2022). Meanwhile, Song et al. presented a novel attention-long short-term memory (A-LSTM) to extract more discriminative features from EEG sequences. A-LSTM shows advanced performance on the MPED dataset proposed in the same paper (Song et al. 2019). In addition, Li et al. proposed a graph-based multi-task self-supervised learning model (GMSS), which integrates multiple self-supervised tasks to learn more general representations for EEG emotion recognition. The experimental results of GMSS on SEED, SEED-IV, and MPED datasets show its advanced performance in learning more discriminative and available features for EEG emotional signals (Li et al. 2022). Zheng et al. introduced deep belief networks (DBNs) to investigate the critical frequency bands and channels of EEG signals. The experiment results show that the 4th, 6th, 9th, and 12th channels and the Gamma band are more important in emotion recognition (Zheng and Lu 2015). Although the above methods have achieved advanced performance in EEG emotion recognition tasks, due to the massive differences in the distribution of training and test data in practical applications, these methods are disabled to perform well.

Transfer Learning in EEG Emotion Recognition

Considering that the EEG signals in cross-subject experiments have a considerable domain shift of data distribution, numerous transfer learning methods have been widely used in cross-subject EEG emotion recognition to overcome the significant distribution divergence of EEG signals among individuals. For example, Li et al. proposed a multisource transfer learning method, which regards the existing subjects as sources and the new subject as a target to realize style transfer mapping (Li et al. 2020). Sun et al. proposed a dual-branch dynamic graph convolution-based adaptive transformer feature fusion network with adapter-finetuned transfer learning (DBGC-ATFFNet-AFTL) for EEG emotion recognition. They utilized the transfer learning method to integrate the different domain features and achieved

promising performance in cross-subject emotion recognition on three datasets (Sun et al. 2022). Peng et al. proposed a joint feature adaptation and graph adaptive label propagation model (JAGP) for cross-subject emotion recognition. JAGP successfully implemented the inter-domain migration by extracting and integrating the domain-invariant features (Peng et al. 2022). Li et al. proposed a novel bi-hemispheres domain adversarial neural network (BiDANN) for EEG emotion recognition. Inspired by the asymmetry of the left and right hemispheres in the emotional functional regions of the brain, BiDANN maps the EEG signals of the left and right hemispheres to the discriminative feature spaces, so that the model can easily classify the data representations on SEED database. (Li et al. 2018). Meanwhile, Li et al. also proposed a transferable attention neural network (TANN) for EEG emotion recognition. TANN is based on the local and global attention mechanism to learn the discriminative information from emotional EEG signals. Extensive experiments on SEED, SEED-IV, and MPED datasets demonstrate the superior performance of TANN (Li et al. 2021). However, the performance of these existing methods decreases significantly when dealing with cross-data EEG emotion recognition tasks. We will compare the representative methods among them with the proposed method in Section .

Proposed Method for Emotion Recognition

To specify the proposed method clearly, we depict the E²STN framework in Fig. 2. The network aims to reorganize the emotional content information of the source domain and the statistical characteristic style of the target domain to obtain new stylized source domain EEG samples, and finally realize the cross-dataset EEG emotion recognition task. We adopt three modules to achieve this goal, i.e., transfer module, discriminative prediction module, and transfer evaluation module. The transfer module is to obtain emotional EEG representations that contain affective content information of the source domain and statistical characteristics style of the target domain. Subsequently, the original and stylized source samples are fed into the discriminative prediction module for cross-dataset EEG emotion recognition. Meanwhile, the transfer evaluation module extracts multi-scale spatio-temporal features of the stylized EEG samples to construct the multi-dimensional losses constraining the process of emotional EEG style transfer. In the following, we introduce the details of the proposed E²STN model.

Obtaining Stylized Emotional EEG Samples

To obtain emotional EEG samples that contain dynamic content information of the source domain and statistical characteristics style of the target domain, we should decompose the transfer into two steps. The first step is to construct transfer encoders corresponding to the source and target domains to capture the global dependencies in the domain-specific information of different fields (i.e., the emotional content of the source domain and the style characteristics of the target domain), respectively. Inspired by the Transformer method (Vaswani et al. 2017), the encoders of E²STN assign dynamic weights to different EEG channels through

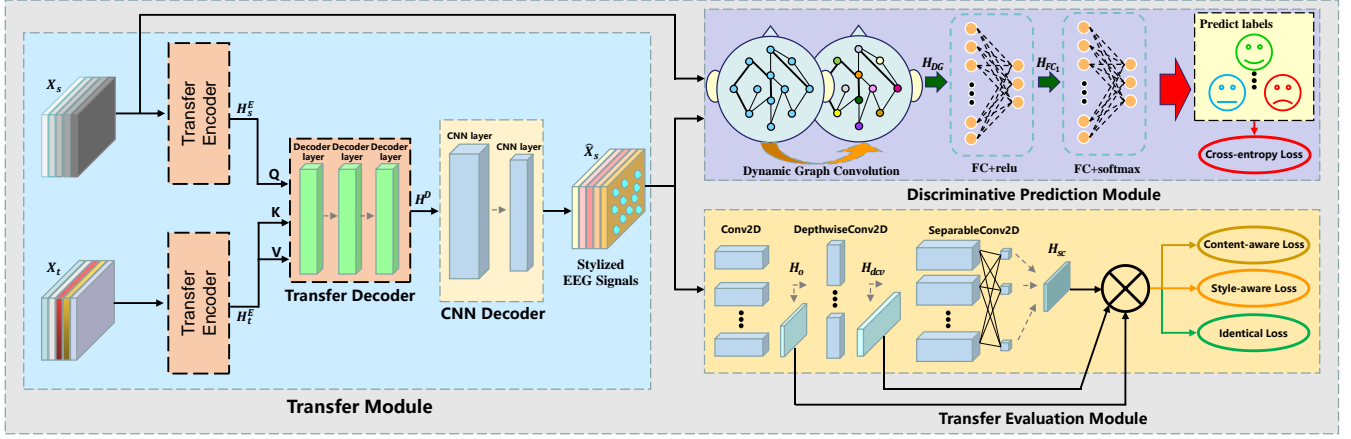


Figure 2: Framework of E^2STN . The transfer module is applied to obtain emotional EEG representations that contain affective content information of the source domain and statistical characteristics style of the target domain. The discriminative prediction module receives stylized and source domain emotional EEG samples for cross-dataset EEG emotion recognition. Meanwhile, the transfer evaluation module progressively extracted spatio-temporal information from the stylized EEG samples to construct the multi-dimensional losses constraining the process of emotional EEG style transfer.

the multi-head self-attention layer, which selects the more important electrode dependencies in the specific domain. The dynamic dependencies with domain-specific information have stronger capabilities in representing their corresponding domain characteristics. The second key step of transfer is to fuse source domain content information and target domain style information in the decoder to obtain stylized source emotional EEG features. The decoder iteratively fuses content and style information by the multi-layer structure, which applies the target domain style to the source domain EEG features. And the residual connection method in the decoder layer ensures that the content information of the source domain will not be distorted.

Specifically, the raw EEG signals are first decomposed into five frequency bands, namely δ band (1–4 Hz), θ band (4–8 Hz), α band (8–14 Hz), β band (14–30 Hz) and γ band (30–50 Hz). The emotional EEG samples corresponding to the source and target domains, respectively, are denoted as $\mathbf{X}_s \in \mathbb{R}^{C \times B}$ and $\mathbf{X}_t \in \mathbb{R}^{C \times B}$, where C is the number of EEG channels and B is the number of frequency bands. Subsequently, two encoders extract the domain-specific information from their corresponding source and target domain EEG features, respectively. The encoder layer structure is depicted in Fig. 3 (a). The emotional EEG samples of the source domain \mathbf{X}_s are first encoded into query (\mathbf{Q}), key (\mathbf{K}), and value (\mathbf{V}) vectors, as shown in formula 1.

$$\mathbf{Q}_s^E = \mathbf{X}_s \mathbf{W}_s^q, \mathbf{K}_s^E = \mathbf{X}_s \mathbf{W}_s^k, \mathbf{V}_s^E = \mathbf{X}_s \mathbf{W}_s^v, \quad (1)$$

where $\mathbf{W}_s^q, \mathbf{W}_s^k, \mathbf{W}_s^v \in \mathbb{R}^{B \times m}$ are trainable linear projection matrices. To enable the encoder to pay attention to the information from different channels, $\mathbf{Q}_s^E, \mathbf{K}_s^E,$ and \mathbf{V}_s^E vectors are divided into several attention heads, that $\mathbf{Q}_s^E, \mathbf{K}_s^E, \mathbf{V}_s^E \in \mathbb{R}^{h \times C \times p}$, where $h = \frac{m}{p}$ is the number of attention heads. Then the multi-head self-attention (MSA) can be calculated by:

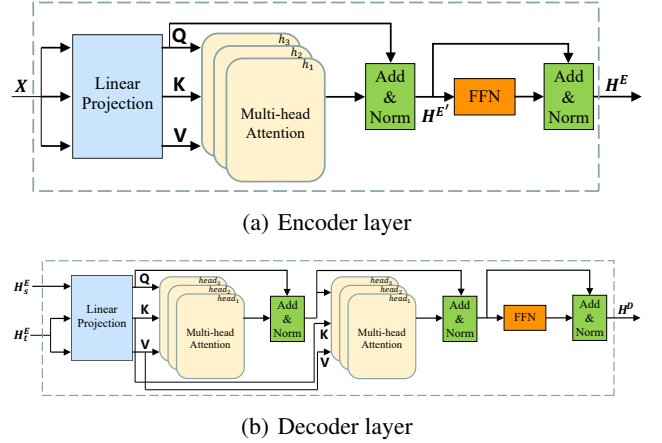


Figure 3: Architecture of encoder and decoder layer in transfer module.

$$\mathbf{M}_s^E = [h_1, \dots, h_h] \mathbf{W}_s^O \in \mathbb{R}^{C \times m}. \quad (2)$$

To preserve domain-specific information, the MSA matrix is added with the Q vector and followed by layer normalization, which can be expressed as:

$$\mathbf{H}_s^{E'} = LN(\mathbf{M}_s^E(\mathbf{Q}_s^E, \mathbf{K}_s^E, \mathbf{V}_s^E) + \mathbf{Q}_s^E), \quad (3)$$

$$\mathbf{H}_s^E = LN(F(\mathbf{H}_s^{E'}) + \mathbf{H}_s^{E'}) \in \mathbb{R}^{C \times m}, \quad (4)$$

$$F(x) = \max(0, x \mathbf{W}_1 + \mathbf{b}_1) \mathbf{W}_2 + \mathbf{b}_2, \quad (5)$$

where $\mathbf{W}_1, \mathbf{W}_2$ are trainable weight matrices, and $\mathbf{b}_1, \mathbf{b}_2$ are trainable bias matrices. Similarly, we can easily obtain the domain-specific features of the target domain \mathbf{H}_t^E .

To fuse the emotional content information of the source domain and the statistical characteristic style of the target domain, we construct a three-layer Transformer decoder, which applies the style of the target domain to the emotional features of the source domain in a progressive manner. The structure of single decoder layer is shown in Fig. 3 (b). The source domain features \mathbf{H}_s^E containing the emotional content information of the source domain are the main objects of transfer, which are used as query vectors for the first decoder layer. To make the source features more similar to the target domain style, the target domain features \mathbf{H}_t^E are used as key and value vectors of the first decoder layer, which calculates a similarity matrix with the query vectors to weight the emotional content features \mathbf{H}_s^E . Specifically, we obtain \mathbf{Q}_1^D , \mathbf{K}_1^D , and \mathbf{V}_1^D through the linear projection, as shown in formula (6).

$$\mathbf{Q}_1^D = \mathbf{H}_s^E \mathbf{W}_q^D, \mathbf{K}_1^D = \mathbf{H}_t^E \mathbf{W}_k^D, \mathbf{V}_1^D = \mathbf{H}_t^E \mathbf{W}_v^D. \quad (6)$$

Following, two MSA layers and one FFN are employed in the first decoder layer with residual connections. The output of the first decoder layer continues to be fed to the second decoder layer, and so on. Therefore, we can easily derive the output $\mathbf{H}^D \in \mathbb{R}^{C \times m}$ of the Transformer decoder through formulas (3), (4), and (5).

To restore the dimension of the stylized features, we employ a two-layer CNN decoder to refine the output of the transformer decoder \mathbf{H}^D . Therefore, we can reshape the stylized EEG features $\mathbf{H}^D \in \mathbb{R}^{C \times m}$ as generated stylized EEG samples $\hat{\mathbf{X}}_s \in \mathbb{R}^{C \times B}$.

Obtaining Discriminative Features and Predictions

After obtaining the stylized source-domain EEG samples, we construct a dynamic graph network to extract deep features, which enables E²STN to learn discriminative features from the original and stylized source samples. The source EEG samples \mathbf{X}_s and the corresponding stylized EEG samples $\hat{\mathbf{X}}_s$ are jointly fed into the discriminative prediction module for obtaining discriminative features and predictions. Concretely, the data-driven graph is represented as $\mathcal{G} = (\mathcal{V}, \mathcal{E})$ according to the standard symbol representation in graph theory, where $\mathcal{V} = \{v_i\}_{i=1}^n$ represents the set of n electrodes of the EEG samples, and $(v_i, v_j) \in \mathcal{E}$ denotes the connection weight between electrodes v_i and v_j in the EEG samples. The relationship between the electrodes is characterized as an adjacency matrix $\mathbf{G} \in \mathbb{R}^{n \times n}$ in the E²STN. The graph connection \mathbf{G} changes adaptively with the input samples \mathbf{X}_s and $\hat{\mathbf{X}}_s$. To make \mathbf{G} contain the intra-channel spatial information and frequency band information, two trainable matrices $\mathbf{W}_s \in \mathbb{R}^{C \times C}$ and $\mathbf{W}_f \in \mathbb{R}^{B \times (C \times B)}$ are multiplied left and right by input features, respectively, which can be expressed as follows:

$$\mathbf{G} = \text{ReLU}[(\mathbf{W}_s \mathbf{X} + \mathbf{B}) \mathbf{W}_f] \in \mathbb{R}^{C \times (C \times B)}, \quad (7)$$

where $\hat{\mathbf{X}}_s = [\mathbf{X}_s, \hat{\mathbf{X}}_s] = \{x_1, \dots, x_t, \dots\}$, ReLU is applied to the output to guarantee non-negative elements, the bias matrix $\mathbf{B} \in \mathbb{R}^{C \times B}$ is used to increase the flexibility

of graph structure representation. Then, the adjacency matrix \mathbf{G} is reshaped into B adjacency matrices, i.e., $\mathbf{G} = [\mathbf{G}_1^*, \dots, \mathbf{G}_B^*] \in \mathbb{R}^{C \times C \times B}$, to represent graphs in B frequency bands.

To avoid the high computational complexity of direct graph Fourier transform based on graph filtering theories, we adopt Chebyshev polynomials to approximate the graph convolution operation (Kipf and Welling 2017). Let $\varphi_k(\mathbf{G}) = \mathbf{G}^k$ denotes the k -order polynomial of the adjacency matrix \mathbf{G} . Therefore, the high-level features extracted by the dynamic GCN can be expressed as follows:

$$\mathbf{H}_{\text{DG}} = \mathcal{G} * \mathcal{F} = \sum_{k=0}^{K-1} \varphi_k(\mathbf{G}) \mathbf{X} \in \mathbb{R}^{C \times F}, \quad (8)$$

where $\varphi_k(\mathbf{G})$ is the k -th level graph, F is the output dimension for the graph convolution operation.

Subsequently, the discriminative prediction module, as the supervision term of the E²STN, applies two fully connected (FC) layers to predict the class labels. *ReLU* activation function is adopted to the first FC layer, and the second FC layer with *softmax* activation function is used to calculate the classification probability. Therefore, the output of the second FC layer $\mathbf{H}_{\text{FC}} = \{o_1, \dots, o_p\} \in \mathbb{R}^{1 \times P}$ can be easily deduced, where P is the output dimension of the FC layer. Then, the discriminative predictions from the softmax layer for emotion recognition can be expressed as follows:

$$\mathbf{Y}(p|x_t) = \exp(o_p) / \sum_{i=1}^P \exp(o_i), \quad (9)$$

where $\mathbf{Y}(p|x_t)$ denotes the predicted probability that the input sample x_t belongs to the p th class in the discriminative prediction module. Consequently, labels l_t of sample x_t are predicted as follows:

$$l_t = \arg \max_p \mathbf{Y}(p|x_t). \quad (10)$$

Consequently, the cross-entropy loss function of E²STN to achieve cross-dataset EEG emotion recognition can be expressed as:

$$L_{ce} = \sum_{t=1}^{M_1} \sum_{p=1}^P -\tau(l_g, l_t) \times \log \mathbf{Y}(p|x_t), \quad (11)$$

$$\tau(x, y) = \begin{cases} 1, & \text{if } x = y \\ 0, & \text{otherwise} \end{cases}. \quad (12)$$

Here, l_g represents the ground-truth label of sample x_t ; M_1 is the number of training samples.

Multi-objective Joint Optimization

To optimize stylized emotional EEG samples, we specially propose a transfer evaluation module to constrain the style transfer process. We mainly consider three factors in the emotional style transfer process, and thus construct three corresponding losses, namely content-aware loss L_c , style-aware loss L_s , and identity loss L_{id} . The first important

point to consider is to preserve the emotional content information of the source domain during the transfer process. We regard the features extracted by the convolutional layer as containing the content information of the corresponding domain (Gatys, Ecker, and Bethge 2016). Therefore, the content-aware loss is built from the features extracted by three unique convolutional layers in the transfer evaluation module, which can be expressed as:

$$L_c = \frac{1}{3} \sum_{i=1}^3 \left\| f_i(\hat{\mathbf{X}}_s) - f_i(\mathbf{X}_s) \right\|_2, \quad (13)$$

where $f_i(\cdot)$ denotes the convolution operation function of the i -th layer in the transfer evaluation module, and $\|\cdot\|_2$ represents the ℓ_2 -norm.

The second point that cannot be ignored in the transfer process is that the style characteristics of the stylized emotional EEG samples should be as similar as possible to those of the target domain. The Gram matrix of the features extracted by the convolutional layer is regarded as the statistical characteristics of the target domain (Gatys, Ecker, and Bethge 2016). Therefore, We can also construct the style-aware loss for the target domain by the statistics (e.g., mean and variance) of each convolutional layer in the transfer evaluation module.

$$L_s = \frac{1}{3} \sum_{i=1}^3 \left(\left\| \mu(f_i(\hat{\mathbf{X}}_s)) - \mu(f_i(\mathbf{X}_t)) \right\|_2 + \left\| \sigma(f_i(\hat{\mathbf{X}}_s)) - \sigma(f_i(\mathbf{X}_t)) \right\|_2 \right), \quad (14)$$

where $\mu(\cdot)$ and $\sigma(\cdot)$ denote the mean and variance of the features, respectively.

In the last point, considering maintaining more accurate content and style information in self-style transfer, we propose an identity loss to ensure the undistorted stylized EEG samples during the progressive transfer process. Specifically, to ensure the lossless and unbiased transfer of emotional EEG samples, we input the same sample \mathbf{X}_s (\mathbf{X}_t) into the source and target domain, and the obtained stylized emotional EEG sample $\hat{\mathbf{X}}_{ss}$ ($\hat{\mathbf{X}}_{tt}$) should be identical to the \mathbf{X}_s (\mathbf{X}_t). Hence, the identity loss L_{id} can be defined as:

$$L_{id} = \frac{1}{3} \sum_{i=1}^3 \left(\left\| f_i(\hat{\mathbf{X}}_{ss}) - f_i(\mathbf{X}_s) \right\|_2 + \left\| f_i(\hat{\mathbf{X}}_{tt}) - f_i(\mathbf{X}_t) \right\|_2 \right), \quad (15)$$

To make the features extracted by the multi-layer convolutional layers in the transfer evaluation module contain multi-dimensional and multi-scale spatio-temporal information, we employ three distinct convolution kernels to construct the convolutional network. The first 2D convolutional layer explores the latent relationship between key bands of stylized EEG features, and $\mathbf{H}_c \in \mathbb{R}^{C \times B \times F_1}$ denotes the overall output feature of the 2D convolution operation, where F_1 is the number of convolutional filters. Subsequently, the depthwise convolution is used to learn the spatial information of stylized EEG features. The depth feature $\mathbf{H}_{dc} \in \mathbb{R}^{1 \times B \times (F_1 * D)}$ can be simply derived, where D is a depth parameter that

controls the number of spatial filters in the convolution operation. In the last layer, separable convolution is the extension of depthwise convolution. On the basis of depthwise convolution, F_2 pointwise convolutions are performed to optimally merge the spatial features. Therefore, the feature \mathbf{H}_{dc} is further compressed in the channel dimension, $\mathbf{H}_{sc} \in \mathbb{R}^{1 \times B \times F_2}$. \mathbf{H}_c , \mathbf{H}_{dc} , and \mathbf{H}_{sc} correspond to the features extracted by each convolutional layers in formulas (13), (14), and (15), respectively.

Finally, the transfer losses in the transfer evaluation module and the cross-entropy loss in the discriminative prediction module together form a multi-objective joint optimization loss function L .

$$L = \lambda L_c + \mu L_s + \nu L_{id} + \xi L_{ce}, \quad (16)$$

where λ, μ, ν, ξ are hyper-parameters used to control the proportion between the optimization loss functions. The E²STN is optimized by iteratively minimizing L , and the emphasis on transferring tasks and classification tasks is achieved by adjusting the hyperparameters. The procedure used to train the E²STN is presented in Algorithm 1 of Appendix A.

Experiments

Experimental Settings

Datasets SEED (Zheng and Lu 2015) is a commonly used emotion EEG dataset published by SJTU, which contains 15 subjects (7 males and 8 females) in total. Each subject in SEED was asked to attend 3 different sessions. During each session, 3 different kinds of emotional film clips (i.e., positive, neutral and negative emotions) were played in proper order. There are 5 film clips for each kind of emotion, that is, a total of 15 trials (approximately 3400 samples) are included in one session. In each session, The EEG signals and eye movements were collected with the 62-channel ESI NeuroScan System¹ and SMI eye-tracking glasses². The locations of the EEG electrodes are based on the international 10–20 system. The EEG data was downsampled to 200 Hz and divided into 1-s segments. The differential entropy (DE) features extracted from the downsampled EEG signals with 1-second sliding window were used as training samples.

SEED-IV (Zheng et al. 2018) contains 15 subjects in total. Similarly, each subject was required to perform three different sessions, but 4 different kinds of emotion were triggered in each session (i.e. happy, sad, fear, and neutral). There are 6 film clips for each kind of emotion, that is, a total of 24 trials are included in one session. The dataset contains EEG and eye movement data, among which the EEG data are collected using a 62-channel ESI neuroscan system. The locations of the EEG electrodes are based on the international 10–20 system. Each session was divided into 1-s segments as a training sample. The DE features at five frequency bands were extracted from all training samples.

¹<https://compumedicsneuroscan.com/>

²<https://www.smivision.com/eye-tracking/product/eye-tracking-glasses/>

The MPED (Song et al. 2019) collects four modal physiological signals: EEG, galvanic skin response, respiration, and electrocardiogram (ECG). 30 subjects are requested to watch 28 videos, which are divided into 7 categories: joy, funny, anger, fear, disgust, sadness, and neutral emotion. Herein, only the EEG data were used for emotion recognition. To remove the noise and artifacts, a 5-order Butterworth filter was used to filter EEG data at 1-100 Hz. The processed data were decomposed into five frequency bands with a slide non-overlapping window of 1-s, and its 256-point STFT features were extracted at the same time.

Experiment protocol The purpose of this paper is to study the cross-dataset EEG emotion recognition tasks. Therefore, following the principles of previous experiments, we set up groups of cross-dataset EEG emotion recognition comparison experiments. Table 1 summarizes the setup details of the cross-dataset EEG emotion recognition experiments. The SEED dataset, which has the fewest categories of emotions of the three datasets we adopted, contains three categories: positive, negative, and neutral. consequently, to ensure the category balance of the training samples, we select the neutral, sad, and happy emotions as the emotional EEG transfer objects for SEED-IV dataset, and neutral, sad, and joy emotions for MPED dataset. The samples of all subjects from one dataset are regarded as source domain data, and the ones in another dataset are used as target domain data. In this way, we can obtain six groups for 3-category cross-dataset EEG emotion recognition experiments, and two groups for 4-category cross-dataset EEG emotion recognition experiments. The eight groups of cross-dataset EEG emotion recognition experiments are denoted as 'MPED³ → SEED³', 'MPED³ → SEED-IV³', 'SEED-IV³ → MPED³', 'SEED-IV³ → SEED³', 'SEED³ → MPED³', 'SEED³ → SEED-IV³', 'MPED⁴ → SEED-IV⁴', and 'SEED-IV⁴ → MPED⁴', respectively.

Experiment Results

3-category cross-dataset EEG emotion recognition To evaluate the performance of our model in cross-dataset EEG emotion recognition, we conduct extensive experiments using three datasets, namely SEED, SEED-IV, and MPED. To compare the proposed E²STN with the other advanced methods of EEG emotion recognition, we also conduct the same experiments using six other methods: linear SVM (Suykens and Vandewalle 1999), A-LSTM (Song et al. 2019), IAG (Song et al. 2020a), GECNN (Song et al. 2022), BiDANN (Li et al. 2018), and TANN (Li et al. 2021). We quote or reproduce their results from the literature to ensure a convincing comparison with the proposed method. The mean accuracy (ACC) and standard deviation (STD) are used as the evaluation criteria for all subjects in the test dataset. The experiment results are presented in Table 2. The best result for each row in the Table is highlighted in bold-face.

Table 2 shows that the proposed E²STN model achieves the best performance in cross-dataset EEG emotion recognition experiments, thus verifying the transfer and recognition effectiveness of the proposed method. Specifically,

E²STN performs best on the 'MPED³ → SEED³' task in the the 3-category cross-dataset EEG emotion recognition experiments, with an accuracy rate of 73.51%, which is significantly higher than that of the compared advanced algorithms. Compared with the state-of-the-art domain adaptation method TANN (Li et al. 2021), E²STN improves the accuracy by 09.28% (73.51% vs 64.23%) on the 3-category classification of the 'MPED³ → SEED³' task. For the 'SEED-IV³ → SEED³' experiment, E²STN achieves the highest classification accuracy with the smallest standard deviation, which proves that the proposed method has the best performance and stability. In 'MPED³ → SEED-IV³' and 'SEED³ → SEED-IV³' experiments (i.e., the 4th and 5th columns of Table 2), the recognition performance of the proposed method has declined, which may be due to the reduction of emotional feature discrimination when the SEED-IV dataset collect finer emotion. Meanwhile, the similar classification performance of the two tasks (62.32% vs. 61.24%) proves the effectiveness of the proposed method in eliminating the domain shift problem. Also for the MPED dataset (which contains more emotion categories), the less discrimination between emotions leads to a further decline in model performance (the 6th and 7th columns of Table 2). However, since E²STN considers both the inter-domain differences between datasets and the dynamic connection relationship of the emotional functional regions of the brain, it still has the highest recognition performance compared with other advanced methods.

To verify the confidence of our experimental results, we perform the t-test statistical analysis (Hanusz, Tarasinska, and Zielinski 2016) on each reproduced accuracy result. First, the Shaprow-Wilk test (S-W test) (Semenick 1990) is performed to eliminate the accuracy data that do not follow the normal distribution hypothesis. The statistical analyses are conducted by the SPSS software (IBM SPSS Statistics³), and the significance level of paired t-test (Hanusz, Tarasinska, and Zielinski 2016) is defined as $p < 0.05$. Taking the GECNN method as an example, our proposed E²STN shows significantly better ($p < 0.05$) with it in each cross-dataset task. From this statistical analysis, it can be seen that our proposed method can effectively reduce the inter-domain differences among different datasets and achieve efficient EEG emotion recognition.

To explore which emotion is more easily recognized by the proposed model, we depict confusion matrices based on the results of the E²STN, which are shown in Fig. 4 (1). From this figure, we can have the following observations. Except for the 'SEED³ → MPED³' experiment (Fig. 4 (f)), the recognition accuracy of 'happiness' emotion is higher than that of 'sadness' emotion, with an average of 24.56% higher. This proves 'happiness' is more accessible to distinguish than 'sadness' emotions, indicating that the 'happiness' emotion is more easily induced in different datasets. Furthermore, compared with the 'happiness' emotion, the average accuracy of 'sadness' emotion is 40.38%. The lower recognition accuracy of 'sadness' emotion is because it is easy to be mistaken for the 'neutrality' emotion, especially

³<https://spss.mairuan.com>

Table 1: The details of experimental groups settings for cross-dataset EEG emotion recognition.

Number of emotional categories	The source domain	The target domain	The emotional categories
3-category	MPED ³	SEED ³	neutral, joy, sad
	MPED ³	SEED-IV ³	neutral, joy(happy), sad
	SEED-IV ³	SEED ³	neutral, happy, sad
	SEED-IV ³	MPED ³	neutral, happy(joy), sad
	SEED ³	SEED-IV ³	neutral, happy, sad
	SEED ³	MPED ³	neutral, joy, sad
4-category	MPED ⁴	SEED-IV ⁴	neutral, joy(happy), sad, fear
	SEED-IV ⁴	MPED ⁴	neutral, happy(joy), sad, fear

All labeled training data and unlabeled test data are used for cross-dataset EEG emotion recognition experiments.

Table 2: 3-category cross-dataset classification performance for EEG emotion recognition on SEED, SEED-IV, and MPED.

Method	ACC / STD (%)					
	MPED ³ → SEED ³	SEED-IV ³ → SEED ³	MPED ³ → SEED-IV ³	SEED ³ → SEED-IV ³	SEED-IV ³ → MPED ³	SEED ³ → MPED ³
SVM (Suykens and Vandewalle 1999)	48.94/04.96	23.63/10.28	27.71/02.93	29.47/06.27	33.32/03.08	40.53/04.74
A-LSTM (Song et al. 2019)	47.55/07.46	46.47/08.30	42.59/06.08	58.19/13.73	38.51/03.94	43.80/05.45
IAG (Song et al. 2020a)	60.89*/-	52.84/07.71	58.61/08.28	59.87/11.16	39.67/03.13	40.90*/-
GECNN (Song et al. 2022)	62.90/06.58	58.02/07.03	60.88/06.96	57.25/07.53	38.82/03.52	43.15/03.08
BiDANN (Li et al. 2018)	61.30/09.14	49.24/10.49	57.57/07.60	60.46/11.17	40.16/04.29	43.17/04.72
TANN (Li et al. 2021)	64.23/09.63	58.41/07.16	55.14/09.59	60.75/10.61	37.16/01.69	40.62/04.66
E ² STN	73.51/07.23	60.51/05.41	62.32/06.60	61.24/15.14	40.43/04.49	45.56/04.78

* indicates the results are obtained from the literature. The rest are obtained by our own implementation.

in Fig. 4(a), (b), (d), and (f), which may be because the "sadness" emotion is weakly stimulated in these experiments. For the 'MPED³ → SEED-IV³' and 'SEED³ → SEED-IV³' experiments, we can have similar observation between Fig. 4(c) and (d) with the SEED-IV dataset as the target dataset. Namely, the recognition accuracies of E²STN for the three emotions have the following relationship: 'neutrality' > 'happiness' > 'sadness'. The increase in emotional categories of the SEED-IV dataset may result in more subtle emotional changes thus more difficult to recognize. For the 'SEED³ → MPED³' experiment in Fig. 4(f), the recognition accuracy of the 'sadness' emotion is highest, which is the opposite of the other experiment results. The grander difference in the emotional categories between the SEED and MPED datasets may lead to a more significant recognition of the 'sadness' emotions.

4-category cross-dataset EEG emotion recognition To evaluate the performance of E²STN under more emotional categories, we conduct additional 4-category cross-dataset EEG emotion recognition experiments on SEED-IV and MPED datasets. Similarly, to compare the E²STN with other representative methods in previous studies on EEG emotion recognition, we also conduct the same experiments using the comparison methods, i.e. linear SVM (Suykens and Vandewalle 1999), A-LSTM (Song et al. 2019), IAG (Song et al. 2020a), GECNN (Song et al. 2022), BiDANN (Li et al. 2018), and TANN (Li et al. 2021). We reproduce their results from the literature to ensure a convincing comparison with the proposed method. The mean accuracy (ACC) and standard deviation (STD) of all subjects in the test dataset as the evaluation criteria are shown in Table 3.

Compared with the 3-category cross-dataset EEG emo-

Table 3: 4-category cross-dataset classification performance for EEG emotion recognition on SEED-IV and MPED.

Method	ACC / STD (%)	
	MPED ⁴ → SEED-IV ⁴	SEED-IV ⁴ → MPED ⁴
SVM (Suykens and Vandewalle 1999)	24.62/05.66	24.99/05.05
A-LSTM (Song et al. 2019)	35.80/06.13	34.07/04.55
IAG (Song et al. 2020a)	49.30/05.85	33.92/04.94
GECNN (Song et al. 2022)	50.86/08.30	33.13/02.65
BiDANN (Li et al. 2018)	48.56/07.73	32.21/06.77
TANN (Li et al. 2021)	49.40/07.33	33.73/01.95
E ² STN	53.75/06.82	36.78/04.79

tion recognition, the increase in the number of emotional analogies leads to a decline in the recognition performance of E²STN. For example, in the 'MPED⁴ → SEED-IV⁴' experiment, the average accuracy rate of E²STN is 53.75%; in the 'SEED-IV⁴ → MPED⁴' experiment, the average accuracy rate is 36.78%. However, E²STN still achieves the highest accuracy compared with the other advanced methods. Meanwhile, in the 'MPED⁴ → SEED-IV⁴' experiment, E²STN improves the accuracy by 02.89% compared to the state-of-the-art method GECNN (Song et al. 2022). Similarly, it improves by 02.71% compared with the state-of-the-art method A-LSTM (Song et al. 2019) in the 'SEED-IV⁴ → MPED⁴' task. Consistent with the 3-category cross-dataset EEG emotion recognition experiment, the accuracy of the MPED dataset as the target domain is slightly lower than that of the SEED-IV dataset. This may be because the MPED dataset collects more categories of emotions, so the feature differences between emotions are more subtle, making it difficult to transfer.

For the 4-category cross-dataset EEG emotion recogni-

tion experiments, we also depict the confusion matrices in Fig. 4 (2). For the 'MPED⁴ → SEED-IV⁴' and 'SEED-IV⁴ → MPED⁴' experiments, we can observe from Fig. 4(g) and (h) that the 'happiness' and 'fear' emotions are easier to recognize. They are on average 14.03% (61.69% with 52.53% vs 43.08%) and 18.02% (46.47% with 43.78% vs 27.11%) higher than the 'sadness' emotion, respectively. Meanwhile, the 'sadness' emotion is easily confused with the 'fear' emotion, especially in Fig. 4(h), which is consistent with the neuroscience research (Kragel and LaBar 2016) that negative emotions (such as 'sadness' and 'fear') have quite similar Euclidean distances. In addition, the recognition accuracy of the 'neutrality' emotion in 'MPED⁴ → SEED-IV⁴' experiment is higher than that in 'SEED-IV⁴ → MPED⁴' experiment (54.06% vs 29.12%), which is reflected in the final recognition results (53.75% vs 36.78% in Table 3).

Discussion

Effect of the transfer module To verify the effect of the proposed transfer module, we modify the framework of E²STN to only leave the discriminative prediction module, denoted by E²STN-t. E²STN-t adopts the same experimental protocols as E²STN but trains only with the labeled source domain samples rather than source domain and stylized EEG samples. The experiment results are listed in Table 4 and 5. Compared with E²STN-t, E²STN significantly improves the performance of 3- and 4-category cross-dataset EEG emotion recognition experiments. In Table 4, E²STN improves the recognition accuracy by an average of 05.69%; in Table 5 of the 4-category cross-dataset experiments, the average increase is 04.56%. This proves that stylized emotional EEG samples can effectively improve the performance of E²STN for cross-dataset EEG emotion recognition, and further verifies the effectiveness of the proposed transfer module.

Exploring the importance of emotion-related brain regions To more clearly explore the contribution of different brain functional regions for EEG emotion recognition, we depict the electrode activity maps in Fig. 5. The contribution of each brain region is reflected in the visualization of advanced features \mathbf{H}_{DG} , which is extracted by the dynamic graph convolutional layer in discriminative prediction module. The darker red areas in the figure indicate that higher contributions from corresponding regions of the brain. It can be clearly seen that the frontal and temporal lobes of the brain are activated, which is consistent with existing neuroscience research (Alarcão and Fonseca 2019). This reflects that E²STN extracts the most important emotion-related features in both stylized and source domain EEG samples, further demonstrating the excellent performance of the proposed method for cross-dataset EEG emotion recognition.

Conclusion

In this study, we propose an EEG-based emotion style transfer network, called E²STN, to realize effective cross-dataset EEG emotion recognition. Concretely, we design three modules to accomplish transfer, discriminative prediction, and

evaluation tasks, respectively. The proposed transfer module can effectively reduce the inter-domain differences in the data distribution of different datasets and generate the stylized emotional EEG samples of the target domain. The discriminative prediction module is composed of dynamic graph convolution and fully connected layers, which is jointly trained by the source domain and stylized EEG samples to achieve accurate prediction for cross-dataset experiments. Finally, the transfer evaluation module extracts multi-scale spatio-temporal features of the stylized EEG samples to construct the multi-dimensional losses constraining the process of emotional EEG style transfer. Extensive experiments have proved the effectiveness of our proposed E²STN in cross-dataset EEG emotion recognition tasks. Meanwhile, we have explored the distribution of important brain regions related to emotion, providing a basis for neurophysiology. In future research, we hope to further explore the transfer rules of emotional EEG signals, so as to further improve the performance of cross-dataset EEG emotion recognition.

Table 4: Ablation experiments for 3-category cross-dataset EEG emotion recognition.

Method	ACC / STD (%)					
	MPED ³ → SEED ³	SEED-IV ³ → SEED ³	MPED ³ → SEED-IV ³	SEED ³ → SEED-IV ³	SEED-IV ³ → MPED ³	SEED ³ → MPED ³
E ² STN	73.51/07.23	60.51/05.41	62.32/06.60	61.24/15.14	40.43/04.49	45.56/04.78
E ² STN-t	65.12/08.99	53.70/08.53	55.58/08.39	58.89/14.35	38.28/04.97	37.85/03.71

Table 5: Ablation experiments for 4-category cross-dataset EEG emotion recognition.

Method	ACC / STD (%)	
	MPED ⁴ → SEED-IV ⁴	SEED-IV ⁴ → MPED ⁴
E ² STN	53.75/06.82	36.78/04.79
E ² STN-t	47.39/07.13	34.03/05.36

References

- Alarcão, S. M.; and Fonseca, M. J. 2019. Emotions Recognition Using EEG Signals: A Survey. *IEEE Transactions on Affective Computing*, 10(3): 374–393.
- Fiorini, L.; Mancipopi, G.; Semeraro, F.; Fujita, H.; and Cavallo, F. 2020. Unsupervised emotional state classification through physiological parameters for social robotics applications. *Knowledge-Based Systems*, 190: 105217.
- Gatys, L. A.; Ecker, A. S.; and Bethge, M. 2016. Image Style Transfer Using Convolutional Neural Networks. In *Proceedings of the IEEE Conference on Computer Vision and Pattern Recognition (CVPR)*.
- Guo, H.; and Gao, W. 2022. Metaverse-Powered Experiential Situational English-Teaching Design: An Emotion-Based Analysis Method. *Frontiers in Psychology*, 13: 859159–859159.
- Hanusz, Z.; Tarasinska, J.; and Zielinski, W. 2016. Shapiro–Wilk test with known mean. *REVSTAT-Statistical Journal*, 14(1): 89–100.
- He, Z.; Li, Z.; Yang, F.; Wang, L.; Li, J.; Zhou, C.; and Pan, J. 2020. Advances in multimodal emotion recognition based on brain–computer interfaces. *Brain sciences*, 10(10): 687.
- Katsigiannis, S.; and Ramzan, N. 2018. DREAMER: A Database for Emotion Recognition Through EEG and ECG Signals From Wireless Low-cost Off-the-Shelf Devices. *IEEE Journal of Biomedical and Health Informatics*, 22(1): 98–107.
- Kipf, T. N.; and Welling, M. 2017. Semi-Supervised Classification with Graph Convolutional Networks. arXiv:1609.02907.
- Kragel, P. A.; and LaBar, K. S. 2016. Decoding the Nature of Emotion in the Brain. *Trends in Cognitive Sciences*, 20(6): 444–455.
- Li, J.; Qiu, S.; Shen, Y.-Y.; Liu, C.-L.; and He, H. 2020. Multisource Transfer Learning for Cross-Subject EEG Emotion Recognition. *IEEE Transactions on Cybernetics*, 50(7): 3281–3293.
- Li, Y.; Chen, J.; Li, F.; Fu, B.; Wu, H.; Ji, Y.; Zhou, Y.; Niu, Y.; Shi, G.; and Zheng, W. 2022. GMSS: Graph-Based Multi-Task Self-Supervised Learning for EEG Emotion Recognition. *IEEE Transactions on Affective Computing*, 1–1.
- Li, Y.; Fu, B.; Li, F.; Shi, G.; and Zheng, W. 2021. A novel transferability attention neural network model for EEG emotion recognition. *Neurocomputing*, 447: 92–101.
- Li, Y.; Zheng, W.; Cui, Z.; Zhang, T.; and Zong, Y. 2018. A Novel Neural Network Model based on Cerebral Hemispheric Asymmetry for EEG Emotion Recognition. In *IJ-CAI*, 1561–1567.
- Murugappan, M.; Rizon, M.; Nagarajan, R.; and Yaacob, S. 2010. Inferring of human emotional states using multichannel EEG. *European Journal of Scientific Research*, 48(2): 281–299.
- Peng, Y.; Kong, W.; Qin, F.; Nie, F.; Fang, J.; Lu, B.-L.; and Cichocki, A. 2021. Self-weighted semi-supervised classification for joint EEG-based emotion recognition and affective activation patterns mining. *IEEE Transactions on Instrumentation and Measurement*, 70: 1–11.
- Peng, Y.; Wang, W.; Kong, W.; Nie, F.; Lu, B.-L.; and Cichocki, A. 2022. Joint Feature Adaptation and Graph Adaptive Label Propagation for Cross-Subject Emotion Recognition From EEG Signals. *IEEE Transactions on Affective Computing*, 13(4): 1941–1958.
- Semenick, D. 1990. Tests and measurements: The T-test. *Strength & Conditioning Journal*, 12(1): 36–37.
- Shu, Y.; and Wang, S. 2017. Emotion recognition through integrating EEG and peripheral signals. In *2017 IEEE international conference on acoustics, speech and signal processing (ICASSP)*, 2871–2875. IEEE.
- Song, T.; Liu, S.; Zheng, W.; Zong, Y.; and Cui, Z. 2020a. Instance-Adaptive Graph for EEG Emotion Recognition. In *AAAI-20*.
- Song, T.; Liu, S.; Zheng, W.; Zong, Y.; Cui, Z.; Li, Y.; and Zhou, X. 2021. Variational instance-adaptive graph for EEG emotion recognition. *IEEE Transactions on Affective Computing*.
- Song, T.; Zheng, W.; Liu, S.; Zong, Y.; Cui, Z.; and Li, Y. 2022. Graph-Embedded Convolutional Neural Network for Image-Based EEG Emotion Recognition. *IEEE Transactions on Emerging Topics in Computing*, 10(3): 1399–1413.
- Song, T.; Zheng, W.; Lu, C.; Zong, Y.; Zhang, X.; and Cui, Z. 2019. MPED: A multi-modal physiological emotion database for discrete emotion recognition. *IEEE Access*, 7: 12177–12191.
- Song, T.; Zheng, W.; Song, P.; and Cui, Z. 2020b. EEG Emotion Recognition Using Dynamical Graph Convolutional Neural Networks. *IEEE Transactions on Affective Computing*, 11(3): 532–541.

Sun, M.; Cui, W.; Yu, S.; Han, H.; Hu, B.; and Li, Y. 2022. A Dual-Branch Dynamic Graph Convolution Based Adaptive TransFormer Feature Fusion Network for EEG Emotion Recognition. *IEEE Transactions on Affective Computing*, 13(4): 2218–2228.

Suykens, J. A.; and Vandewalle, J. 1999. Least squares support vector machine classifiers. *Neural Processing Letters*, 9(3): 293–300.

Van der Maaten, L.; and Hinton, G. 2008. Visualizing data using t-SNE. *Journal of machine learning research*, 9(11).

Vaswani, A.; Shazeer, N.; Parmar, N.; Uszkoreit, J.; Jones, L.; Gomez, A. N.; Kaiser, L. u.; and Polosukhin, I. 2017. Attention is All you Need. In Guyon, I.; Luxburg, U. V.; Bengio, S.; Wallach, H.; Fergus, R.; Vishwanathan, S.; and Garnett, R., eds., *Advances in Neural Information Processing Systems*, volume 30. Curran Associates, Inc.

Xiao, G.; Shi, M.; Ye, M.; Xu, B.; Chen, Z.; and Ren, Q. 2022. 4D attention-based neural network for EEG emotion recognition. *Cognitive Neurodynamics*, 1–14.

Zheng, W.; Liu, W.; Lu, Y.; Lu, B.; and Cichocki, A. 2018. EmotionMeter: A Multimodal Framework for Recognizing Human Emotions. *IEEE Transactions on Cybernetics*, 1–13.

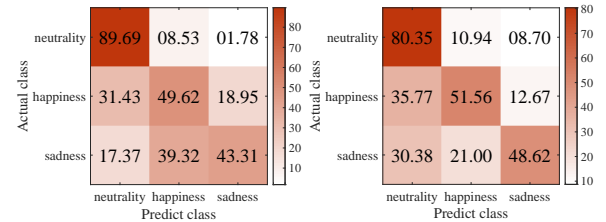
Zheng, W.-L.; and Lu, B.-L. 2015. Investigating critical frequency bands and channels for EEG-based emotion recognition with deep neural networks. *IEEE Transactions on autonomous mental development*, 7(3): 162–175.

Zheng, W.-L.; Zhu, J.-Y.; and Lu, B.-L. 2017. Identifying stable patterns over time for emotion recognition from EEG. *IEEE Transactions on Affective Computing*, 10(3): 417–429.

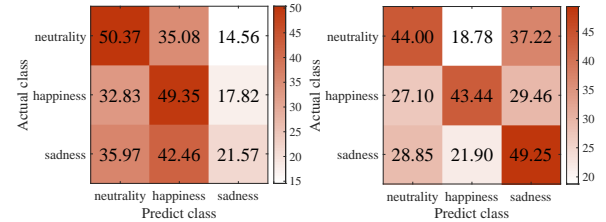
Zhong, P.; Wang, D.; and Miao, C. 2020. EEG-based emotion recognition using regularized graph neural networks. *IEEE Transactions on Affective Computing*, 13(3): 1290–1301.



(a) MPED³ → SEED³ (b) SEED-IV³ → SEED³

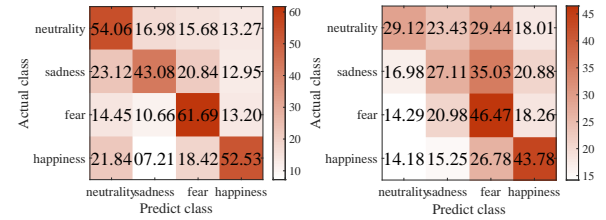


(c) MPED³ → SEED-IV³ (d) SEED³ → SEED-IV³



(e) SEED-IV³ → MPED³ (f) SEED³ → MPED³

(1) 3-category



(g) MPED⁴ → SEED-IV⁴ (h) SEED-IV⁴ → MPED⁴

(2) 4-category

Figure 4: Confusion matrices of E²STN results on cross-dataset experiments.

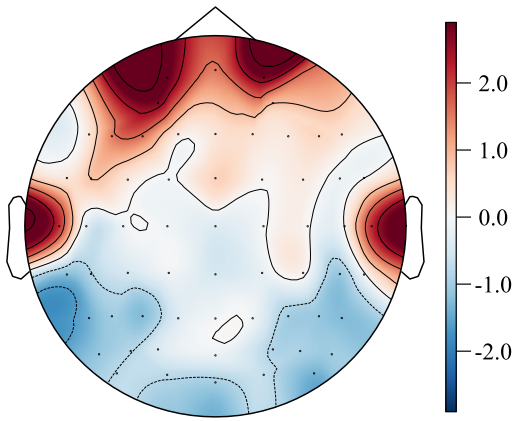


Figure 5: Visualization of H_{DG} distribution in the discriminative prediction module.

Appendix A: Algorithm procedure

Algorithm 1 Procedure of the E²STN model.

Require: Labeled source domain data \mathbf{X}_s , the corresponding class labels \mathbf{Y}_s ; Unlabeled target domain data \mathbf{X}_t .

Ensure:

- 1: Initialize model parameters;
 - 2: **for** each $i \in [0, epochs]$ **do**
 - 3: Calculate $\mathbf{Q}_s^E, \mathbf{K}_s^E, \mathbf{V}_s^E$ with $\mathbf{W}_s^q, \mathbf{W}_s^k, \mathbf{W}_s^v$, and \mathbf{X}_s ;
 - 4: Calculate $\mathbf{Q}_t^E, \mathbf{K}_t^E, \mathbf{V}_t^E$ with $\mathbf{W}_t^q, \mathbf{W}_t^k, \mathbf{W}_t^v$, and \mathbf{X}_t ;
 - 5: Conduct MSA and FFN calculations of the source and target domain, obtain the domain-specific features \mathbf{H}_s^E and \mathbf{H}_t^E from the encoders;
 - 6: **for** each $j \in [1, 3]$ **do**
 - 7: Calculate $\mathbf{Q}_j^D, \mathbf{K}_j^D, \mathbf{V}_j^D$ with $\mathbf{W}_q^D, \mathbf{W}_k^D, \mathbf{W}_v^D, \mathbf{H}_s^E$, and \mathbf{H}_t^E ;
 - 8: Conduct MSA and FFN calculations in the decoder layers, obtain the fused feature \mathbf{H}^D ;
 - 9: **end for**
 - 10: Refine the fused features \mathbf{H}^D by the CNN decoder to obtain the stylized EEG features $\hat{\mathbf{X}}_s$;
 - 11: Make prediction by the discriminative prediction module from the source domain EEG features \mathbf{X}_s and the corresponding stylized EEG features $\hat{\mathbf{X}}_s$, calculate the cross-entropy loss L_{ce} ;
 - 12: Extract multi-dimensional information by the transfer evaluation module, calculate transfer losses L_c, L_s , and L_{id} .
 - 13: Update parameters according to gradient descent algorithm;
 - 14: **end for**
-

Appendix B: Implementation details

Our model is trained on an NVIDIA GeForce RTX 2080Ti GPU, with CUDA 10.1 and cuDNN 7.6.2, in Tensorflow. The number of EEG channels C and frequency bands B are 62 and 5; The parameters in the transfer module are simply set to $d_{model} = 50, h = 10$, and the dimension of the inner-layer in FFN = 256; The parameters in the discriminative prediction module are simply set to $K = 5, F = 128, P = 3$, and the output dimension of the first dense layer = 200; The parameters of in the transfer evaluation module are simply set to $F_1 = 8, D = 8, F_2 = 8$; The hyper-parameters λ, μ, ν, ξ are set to 2, 10, 1, 20, respectively.